Rich Variety of Defects in ZnO via an Attractive Interaction between O Vacancies and Zn Interstitials: Origin of *n*-Type Doping

Yong-Sung Kim*
Korea Research Institute of Standards and Science, P.O. Box 102, Yuseong, Daejeon 305-600, Korea

C. H. Park†
Research Center for Dielectric and Advanced Matter Physics, Department of Physics Education, Pusan National University, Pusan 609-735, Korea

(Received 12 November 2008; published 27 February 2009)

As the concentration of intrinsic defects becomes sufficiently high in O-deficient ZnO, interactions between defects lead to a significant reduction in their formation energies. We show that the formation of both O vacancies and Zn interstitials becomes significantly enhanced by a strong *attractive* interaction between them, making these defects an important source of *n*-type conductivity in ZnO.

DOI: 10.1103/PhysRevLett.102.086403 PACS numbers: 71.55.Gs, 72.80.Ey, 73.61.Ga

It is well known that O-deficient ZnO can easily become *n*-type even without the introduction of any intentional dopants. The mechanisms leading to the *n*-type behavior are, however, still controversial. Even though native defects resulting from this deficiency have been excluded as the main source of the high free electron density, the *n*-type conductivity of ZnO is seen to be closely related to its O deficiency which manifests itself through the formation of O-vacancy (V_O) and/or Zn-interstitial (I_{Zn}) defects.

Theoretical first-principles studies of the formation enthalpies of point defects in ZnO have indicated that neither V_O nor I_{Zn} can lead to a high concentration of free carriers, since the most stable donorlike defect V_O has been shown to be a deep donor and the formation of the I_{Zn} shallow-donor state has been known to be energetically far less favorable than that of V_O when the Fermi level is close to the conduction-band minimum (CBM) [1–7]. On the other hand, hydrogen contamination was proposed to be an important cause of the natural *n* doping [8–10]. Especially, hydrogen was found to be strongly trapped by a V_O, giving a shallow-donor state [10]. A potential problem with this proposal is that a high concentration of electron carriers is still observed even when H contamination is minimized or when H is removed [11–13]. The sample annealed at 1100 °C in Zn vapor had an electron concentration of 1.5×10^{18} cm^{-3}, while the untreated sample had 1.3×10^{17} cm^{-3} [11]. Hydrogen easily diffuses out of ZnO at high temperature, and the H-related hyperfine structure observed in H-contaminated samples from the electron nuclear double-resonance study [14] was not observed in such heat-treated samples [15]. A metastable shallow-donor state of V_O was suggested as an alternative source of the *n* doping [16], but it is still controversial.

As the concentration of defects becomes high, interactions between defects become unavoidable and they need to be taken into account. It is known that donorlike and acceptorlike defects are attracted towards each other through their Coulombic interaction [17]. However, the defect-defect interactions between donorlike defects have been neglected in previous theoretical studies of ZnO, while they were considered in ZnTe for extrinsic *n* doping [18]. In this Letter, we show that there can be a strong *attractive* interaction between two donorlike defects, the deep donor V_O and the shallow donor I_{Zn}. The driving force for the attractive interaction is the quantum mechanical hybridization between the electronic orbitals of their respective deep- and shallow-donor states, which attracts I_{Zn} toward V_O. The interaction significantly lowers the energy of the electronic donor orbital of V_O, as the distance between two defects decreases. The overall effect is a large reduction in the total energy of the system. As a result, the concentration of I_{Zn} can reach a high enough level to explain the high concentration of electron carriers in O-deficient ZnO, even if the Fermi level is close to the CBM.

We performed density functional theory calculations, as implemented in the Vienna *ab initio* simulation package (VASP) code [19,20]. In order to examine interactions between defects, we employ a supercell geometry, in which two defects are located at various sites in the cell, and calculate the variation of the total energy depending on their distance. We consider two low-energy donorlike defects: V_O and I_{Zn}. In *n*-type O-deficient ZnO, the Fermi level is close to the CBM, and the neutral charge state of V_O is stable, since V_O is a deep-donor defect, but the shallow donor I_{Zn} is stable in a (2+)-charge state. Therefore, only interactions between these charge states are focused on in this work. The results of our calculations are shown in Fig. 1, where the variations of formation enthalpies [$\Omega_{\alpha,\alpha'}(r)$] as a function of defect-defect (α-α') separation (r) are shown. The Fermi level is assumed to be located at the V_O deep-donor level.

We first consider interactions between two V_O's and, separately, between two I_{Zn}'s. It is found that the total energy increases as the distance between the defects de-

 © 2009 The American Physical Society

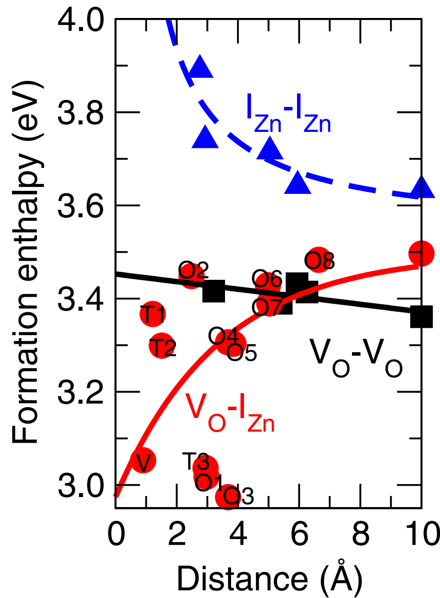

FIG. 1 (color online). Calculated formation enthalpies of V_O-I_{Zn} (●), V_O-V_O (■), and I_{Zn}-I_{Zn} (▲) pairs as a function of the distance. For V_O-I_{Zn}, the corresponding atomic sites are indicated as in Fig. 2.

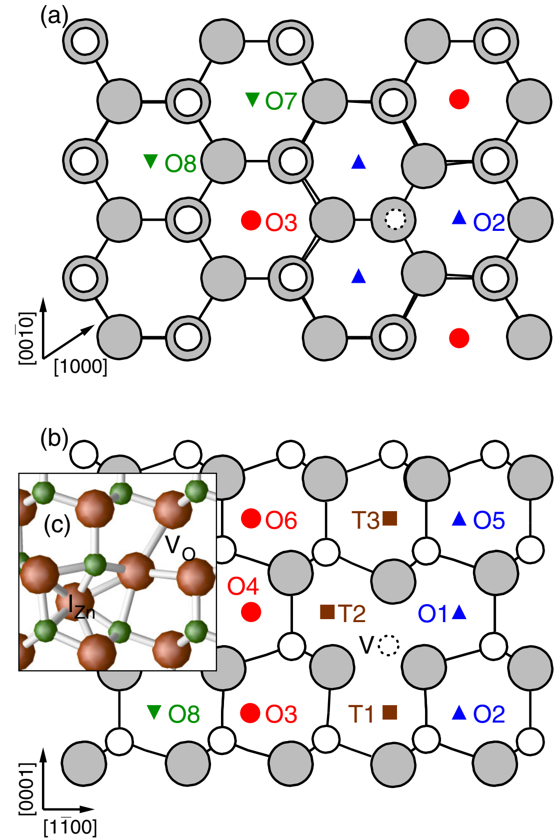

FIG. 2 (color online). Available atomic sites for a I_{Zn} near a V_O shown from the top (along the polar axis) and from the side view. (c) Atomic structure of the most stable V_O-I_{Zn} pair (O3). The large and small atoms are Zn and O, respectively.

creases, indicating a repulsive interaction between same-type defects. As shown in Fig. 1, the energy of two I_{Zn}'s increases sharply as they get closer to each other, whereas that of two V_O's increases slightly. The repulsive interaction between I_{Zn}'s is due to the expected Coulombic repulsion. The variation of the energy is fit well using the screened Coulombic interaction functional $\frac{Z^2e^2}{4\pi\epsilon}\cdot\frac{e^{-r/\lambda}}{r}$, where the fitting parameters are the charge state $Z = 2$, the dielectric constant $\epsilon = 8.65$, and the screening length $\lambda = 1.13$ Å. The weak repulsive interaction between V_O's is related to a strain effect. Between the neutral species, there is no dominant Coulombic interaction. The inward relaxation of neutral V_O induces a tensile strain into the surrounding lattice. In the paired state, the strain does not become fully relaxed.

An interesting finding is that there is a strong attractive interaction between V_O and I_{Zn}. The formation enthalpy of V_O-I_{Zn} pairs as a function of their separation is shown in Fig. 1. The total energy decreases significantly, as the separation becomes smaller, indicating that I_{Zn} is stable with respect to a coupling to an on-site Zn atom surrounding V_O. In Figs. 2(a) and 2(b), the possible sites for I_{Zn} around V_O are indicated: the octahedral interstitial sites (O1–O8), the tetrahedral interstitial sites (T1–T3), and the V_O site (V). The most stable site is the O3 octahedral interstitial site for which the atomic structure is shown in Fig. 2(c). The binding energy is 0.52 eV. There are three equivalent O3 sites around a V_O. When I_{Zn} is trapped just at the oxygen vacancy site V (as an antisite defect), the 0.44 eV binding energy is slightly smaller.

In order to understand the driving force of the attraction between V_O and I_{Zn}, we examined the change of the electronic structure, depending on distance. The electronic structure of the coupled state is significantly modified as the separation between the two defects becomes smaller. It is noted that the defect levels of the V_O (both the occupied a_1 gap state and the unoccupied t_2 state) are lowered while those of I_{Zn} state are raised. The calculated results for the electronic structure are described by the local density of states from the four Zn atoms around V_O and from the I_{Zn} atom, as shown in Figs. 3(a)–3(e). Figure 3(g) describes the lowering of the V_O state as a function of the distance. The lowering is noted to be quantitatively similar to the change of the formation enthalpy in Fig. 1. This indicates that there is a strong interaction between these two defect levels.

The driving force for the attraction originates from the hybridization between the deep-donor state and the shallow-donor state. The change in electronic structure can be simply depicted as in Fig. 3(f). The defect level of the shallow donor I_{Zn} is located inside the conduction bands and the V_O level is located deep within the band gap. Both defect orbitals mainly come from the Zn-4s orbitals. As the distance between the two defects becomes smaller, a

hybridization between the two defect orbitals is induced, as a result of which the lower-lying V_O level is lowered, and the upper I_{Zn} level is pushed up. Since the V_O level is occupied by two electrons while the I_{Zn} level is empty, the hybridization lowers the total energy. As the defect-defect separation becomes smaller, the hybridization becomes stronger. This gives rise to an attractive interaction between the deep- and shallow-donor states. As shown in Fig. 3(g), the change of the V_O level is well fit by an exponential function: $\delta_0 e^{-r/a^*}$, with the fitting parameters $\delta_0 = 0.47$ eV, which is δ at $r = 0$ Å, and $a^* = 4.29$ Å. The wave functions of the defect levels of the donorlike V_O and I_{Zn} can be approximately written by e^{-r/a_V} and e^{-r/a_I}, respectively, where a_V and a_I are the effective Bohr radii of the defect electron densities. The deep level of V_O is localized nearly within the second oxygen nearest neighbor $a_V \sim 5.5$ Å, and the shallow-donor state is delocalized as $a_I = a_0 \epsilon / m_e^* = 20$ Å within the simple effective mass theory, where the Bohr radius $a_0 = 0.53$ Å, the dielectric constant $\epsilon = 8.65$, and the effective mass of the electron $m_e^* = 0.23$. The fitting value of a^* can be obtained from the product of the two wave functions $\langle \psi_V \mid \psi_I \rangle$, with $a_V = 5.5$ Å and $a_I = 20$ Å, i.e., $1/a^* = 1/a_V + 1/a_I = 1/(4.3$ Å$)$. There is just a slight deviation between the lowering of the total energy (Fig. 1) and the V_O level [Fig. 3 (g)] from the fitting curves, which is related to the local strain effect. The closest V_O-I_{Zn} pair (V) shows the largest level drop 0.403 eV [see Figs. 3(e) and 3(g)], and the lowest energy configuration is found at the O3 site, because the O3 interstitial volume is more spacious as it is located behind the inward-relaxed V_O [see Fig. 2(c)], and thus the accommodation of I_{Zn} is easier. While the tensile (V_O-V_O) or compressive (I_{Zn}-I_{Zn}) local strains are accumulated between the same types of defects, the tensile and compressive strains are compensated for V_O-I_{Zn} pairs, giving a further weak attractive interaction. The interaction via orbital hybridization between the defects is more significant than the elastic interaction. Coulombic interaction is not dominant here, since the V_O is neutral in charge.

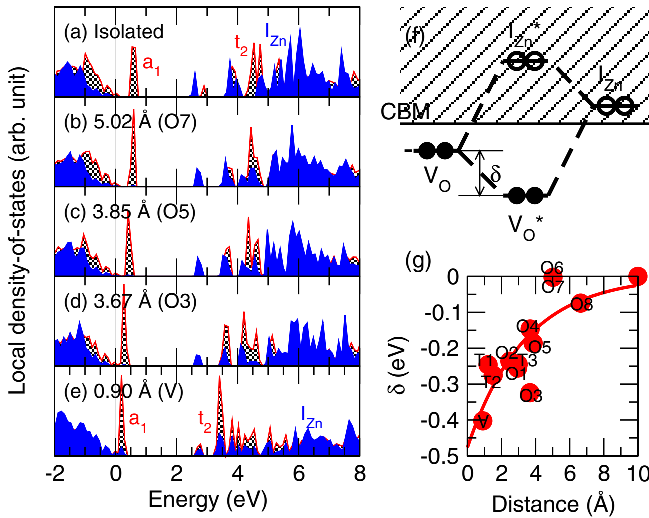

FIG. 3 (color online). Calculated local density of states of electrons near V_O (red) and near I_{Zn} (blue) for (a) the separated V_O and I_{Zn} and for the V_O-I_{Zn} pairs of (b) O7, (c) O5, (d) O3, and (e) V, of which sites are indicated in Fig. 2. (f) Schematic diagram of the defect levels of V_O, I_{Zn}, and V_O-I_{Zn}. V_O^* and I_{Zn}^* denote the V_O and I_{Zn} in the V_O-I_{Zn} pair, respectively. (g) Calculated level drops δ of the V_O state as a function of the distance. The corresponding atomic sites are indicated as in Fig. 2.

The attractive interaction between V_O and I_{Zn} can lead to the coexistence state of both V_O and I_{Zn} rather than the presence of only V_O in O-deficient ZnO. We estimated the concentrations of the V_O-I_{Zn} pair, relatively to isolated defects, and also the Fermi level through the calculations of the formation enthalpies of defects under the thermal equilibrium condition. The average formation enthalpy of a defect α under the interaction with α' defects is calculated by

$$\Omega_\alpha = \Omega_\alpha^0 + \sum_r \sum_{\alpha'} U_{\alpha,\alpha'}(r), \qquad (1)$$

where Ω_α^0 is the formation enthalpy in the isolated state without interaction and $U_{\alpha,\alpha'}(r)$ is the interaction energy between α and α' defects separated by r. In Fig. 1, the calculated $\Omega_{\alpha,\alpha'}(r) = \Omega_\alpha^0 + \Omega_{\alpha'}^0 + U_{\alpha,\alpha'}(r)$ are shown, by which $U_{\alpha,\alpha'}(r)$ can be estimated. For the numerical simplicity, particularly in the limit of extreme high concentrations of defects, we adopt a mean-field concept, and Ω_α can be approximated by $\Omega_\alpha^0 + \sum_{\alpha'} \bar{U}_{\alpha,\alpha'}$, where $\bar{U}_{\alpha,\alpha'} = \int dV U_{\alpha,\alpha'}(r) n_{\alpha'}$ is the mean interaction energy between defect α and α' and $U_{\alpha,\alpha'}(r)$ is approximated by the fitting curves drawn in Fig. 1. Here $n_{\alpha'}$ is the density of a defect α'. When we employed the calculated values for $U_{\alpha,\alpha'}(r)$ shown in Fig. 1, the overall results showed little change. Now we follow a conventional method [21] to determine the concentration of each defect by $n_\alpha = N_0 e^{-\beta \Omega_\alpha}$, the Fermi level ($\varepsilon_F$), and the carrier concentration (n_e) by the charge neutrality condition. N_0 is the number of available sites for defect formation: about 4.68×10^{22} cm^{-3} in ZnO from the theoretical equilibrium lattice constants [20]. The concentration of electron carriers depending on ε_F is determined by $n_e = N_c e^{-(E_c - \varepsilon_F)}$, where E_c is the CBM and $N_c = \frac{1}{4}(\frac{2m_e^*}{\beta \pi \hbar^2})^{3/2}$ is the effective density of electronic states of the CBM [22]. The N_c calculated from a conduction-band electron effective mass of $m_e^* = 0.23$ is 1.4×10^{19} cm^{-3} at 900 K. Since the concentration of hole carriers is minor, so the results are insensitive to the density of the state around the valance band maximum, we used an effective mass of $m_h^* = 0.5$ [23]. The formation enthalpies of the isolated V_O^0 and I_{Zn}^{2+} are 1.68 eV and $2\varepsilon_F$-0.91 eV, respectively, under the Zn-rich condition, where the Zn chemical potential is chosen to be the energy of a Zn atom in the Zn hcp metal [20]. The crystal growth condition

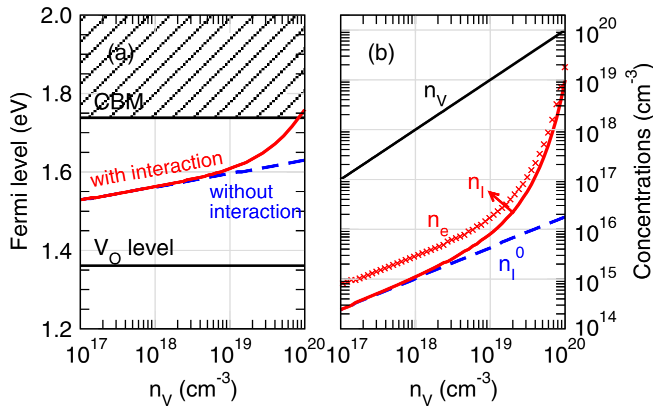

FIG. 4 (color online). (a) Fermi level and (b) equilibrium concentrations of I_{Zn} calculated by considering the defect interactions (red) and neglecting the interactions (blue) as a function of V_O concentrations. Theoretical values of the CBM and the V_O level are indicated in (a). Equilibrium electron carrier concentrations (n_e) are also plotted in (b).

varied between O-rich and Zn-rich conditions is represented by the O chemical potential, which affects the defect concentration.

In Fig. 4, the concentration of I_{Zn} (n_I) and the Fermi level are shown with respect to the concentration of V_O (n_V) at a growth temperature of 900 K. When we neglect the interactions between defects, the Fermi level is calculated to be pinned at a midlevel between the CBM and the V_O level, and n_I is limited to much less than 10^{17} cm^{-3}, as conventionally indicated. When we include the interactions between defects, the result is significantly changed. Under the O-deficient condition, n_I can become close to n_V; i.e., the coexistence of the V_O and I_{Zn} in the O-deficient ZnO becomes remarkable. Since I_{Zn} is a shallow-donor defect, Fermi level can be raised to levels much higher than those expected in the presence of only V_O's, and thus the O-deficient ZnO can be heavily n-type doped. These findings show how the O deficiency itself can be the source of the n-type conductivity in ZnO. When n_V rises up approximately 10^{20} cm^{-3}, where the average distance between V_O's is about 27 Å, n_I can reach about 10^{19} cm^{-3}, and the Fermi level approaches the CBM with an electron carrier concentration n_e of 2×10^{19} cm^{-3}.

Recently, Vlasenko and Watkins have reported the existence of a complex defect consisting of a deep donor V_O and a shallow donor in ZnO through the optical detection of electron paramagnetic resonance (EPR) in electron-irradiated ZnO [24]. They identified an EPR line whose g value is accurately given by the average of the g values of the EPR signals from V_O and a shallow donor. The coincidence was suggested to be the result expected for a closely located defect pair, i.e., V_O and a shallow donor. The pair may be explained by the V_O-I_{Zn} pair reported in this present study. It should be also noted that the defect level of V_O can be deeper below the midgap of ZnO when coupled with I_{Zn} than isolated.

Y. S. K. acknowledges the support of KRCF through the "Development of Advanced Materials Metrology" project and also the support from the KISTI under "The 11th Strategic Supercomputing Support Program." C. H. P. acknowledges the support of the KOSEF grant funded by the Korea government (No. R01-2008-000-21092-0). We also acknowledge Dr. D. J. Chadi for valuable comments.

*Corresponding author.
yongsung.kim@kriss.re.kr
†Corresponding author.
cpark@pusan.ac.kr

[1] A. F. Kohan, G. Ceder, D. Morgan, and C. G. Van de Walle, Phys. Rev. B **61**, 15 019 (2000).
[2] E.-C. Lee, Y.-S. Kim, Y.-G. Jin, and K. J. Chang, Phys. Rev. B **64**, 085120 (2001).
[3] S. B. Zhang, S.-H. Wei, and A. Zunger, Phys. Rev. B **63**, 075205 (2001).
[4] F. Oba *et al.*, J. Appl. Phys. **90**, 824 (2001).
[5] A. Janotti and C. G. Van de Walle, Appl. Phys. Lett. **87**, 122102 (2005).
[6] P. Erhart, A. Klein, and K. Albe, Phys. Rev. B **72**, 085213 (2005).
[7] A. Janotti and C. G. Van de Walle, Phys. Rev. B **76**, 165202 (2007).
[8] C. G. Van de Walle, Phys. Rev. Lett. **85**, 1012 (2000).
[9] C. G. Van de Walle and J. Neugebauer, Nature (London) **423**, 626 (2003).
[10] A. Janotti and C. G. Van de Walle, Nature Mater. **6**, 44 (2007).
[11] L. E. Halliburton *et al.*, Appl. Phys. Lett. **87**, 172108 (2005).
[12] K. Ogata *et al.*, J. Cryst. Growth **214–215**, 312 (2000).
[13] Z. Q. Chen *et al.*, J. Appl. Phys. **94**, 4807 (2003).
[14] D. M. Hofmann *et al.*, Phys. Rev. Lett. **88**, 045504 (2002).
[15] L. E. Halliburton (private communication).
[16] S. Lany and A. Zunger, Phys. Rev. B **72**, 035215 (2005).
[17] S. Limpijumnong, S. B. Zhang, S.-H. Wei, and C. H. Park, Phys. Rev. Lett. **92**, 155504 (2004).
[18] A. Janotti, S.-H. Wei, and S. B. Zhang, Appl. Phys. Lett. **83**, 3522 (2003).
[19] G. Kresse and D. Joubert, Phys. Rev. B **59**, 1758 (1999).
[20] See EPAPS Document No. E-PRLTAO-102-068910 for further calculational details and some results for isolated defects. For more information on EPAPS, see http://www.aip.org/pubservs/epaps.html.
[21] S. B. Zhang and J. E. Northrup, Phys. Rev. Lett. **67**, 2339 (1991).
[22] N. W. Ashcroft and N. D. Mermin, *Solid State Physics* (Saunders College, Philadelphia, 1976), p. 574.
[23] W. R. L. Lambrecht *et al.*, Phys. Rev. B **65**, 075207 (2002).
[24] L. S. Vlasenko and G. D. Watkins, Phys. Rev. B **71**, 125210 (2005).